IEEE Access
Multidisciplinary | Rapid Review | Open Access Journal

Received November 15, 2018, accepted December 28, 2018, date of publication January 3, 2019, date of current version January 23, 2019.

Digital Object Identifier 10.1109/ACCESS.2018.2890717

Three-Dimensional Density Estimation of Flame Captured From Multiple Cameras

GANG-JOON YOON[1], HYEYOUN CHO[2], YONG-YUK WON[3], (Member, IEEE), AND SANG MIN YOON[2]

[1]National Institute for Mathematical Sciences, Daejeon 34047, South Korea
[2]HCI Lab, College of Computer Science, Kookmin University, Seoul 02707, South Korea
[3]Department of Electronics Engineering, Myongji University, Seoul 449718, South Korea

Corresponding author: Sang Min Yoon (smyoon@kookmin.ac.kr)

The work of G.-J. Yoon was supported by the National Institute for Mathematical Sciences. The work of S. M. Yoon was supported in part by the National Research Foundation of Korea under Grant 2015R1A5A7037615 and in part by the Basic Science Research Program (3D Reconstruction of High-Resolution Optical Microscopy Software Development) through the National Research Foundation of Korea, Korean Ministry of Education, under Grant NRF-2016R1D1A1B04932889.

ABSTRACT Optical combustion measurement and analysis systems using multiple sensors have received considerable attention. In particular, the image-based flame 3D reconstruction approaches using computerized tomography have been widely applied for the flame 3D reconstruction from a set of views by constructing the optimized linear combinations of the 3D scene and projected images. Previous techniques were easily computed but were weak against noise and blurring due to the underlying least square-based loss function. This paper presents a 3D density flame reconstruction method, captured from the sparse multi-view images, as a constrained optimization problem between the flame and its projected images. For effective estimation of the flame with a complicated structure in an arbitrary viewpoint, we extract the 3D candidate region of the flame and, then, estimate the density field using the compressive sensing. The objective function is a linear combination of the photo consistency cost and sparsity regularization terms, which avoids blurring in the reconstruction. The proposed approach is a powerful matrix factorization method with each voxel represented as a linear combination of a small number of basis vectors. The approach also effectively simplifies the reconstruction process and provides the whole 3D density field in one step. The experimental results verify that the proposed 3D density estimation performs favorably from the few flame images.

INDEX TERMS Combustion, compressive sensing, image-based reconstruction, three-dimensional reconstruction.

I. INTRODUCTION

Combustion measurement has attracted considerable attention in diverse areas to analyze pressure, optical signal control, and data acquisition and visualization by revealing key control parameters and their effects in the flame's region of interest [1]–[5]. In particular, laser based three-dimensional (3D) flame reconstruction [4], [5] has been widely applied to effectively represent combustion characteristics, but these techniques are usually based on either line of sight measurements, or can only provide 2D results, mismatching the 3D nature of turbulent flame. They also do not adequately consider human visual perception characteristics. To compensate for laser based the disadvantages, image based combustion analysis and visualization [1]–[3] provide better human visual perception characteristics with lower equipment costs.

Three-dimensional view synthesis and understanding from sparse multi-view images is an important topic with a wide range of applications including dynamic image based rendering, view interpolation, 3D reconstruction and understanding, realistic 3D static model reconstruction, etc [6]. Although numerous 3D view synthesis approaches have been proposed, most approaches focus on 3D reconstruction of the surface of an opaque object based on the Lambertian reflectance assumption. Substantial progress has been made on 3D view synthesis of opaque objects, but there has been little consideration of 3D view synthesis for semitransparent (e.g. flame and smoke) and transparent (e.g. glass and water) objects. The objects types are distinguished as follows:

- opaque objects fully reflect light at the object surface according to the objects bidirectional radiance distribution function (BRDF);

- semitransparent objects partially reflect, absorb, and transmit light; and
- transparent objects transmit all incoming light [7].

Since the natural world is composed of opaque, semitransparent, and transparent objects, we consider the less studied problem of 3D view synthesis of semitransparent objects, such as flame [8], [9].

The traditional image based modeling and rendering approach to 3D flame view synthesis and density estimation uses photo consistency as a check condition, but cannot be blindly applied to semitransparent objects because it leverages diffuse and scattering reflectance, and light scattering, which are Lambertian reflectance characteristics for opaque objects. Since semitransparent objects do not have Lambertian reflectance, the BRDF cannot be used.

In contrast, the relationship between the 3D flame and refraction-free projected images can be expressed using a general model of radiative transfer,

$$I = \int_0^L D(t)\tau(t)J(t)dt + I_{bg}\tau(L), \tag{1}$$

where I is the intensity of a pixel of the projected image, which integrates radiance from the luminous flame along the ray through the pixel and incorporates background radiance; $D(t)$ is the density field along that ray; J is the total emission per unit mass; L defines the interval $[0, L]$ along the ray where the field is nonzero; I_{bg} is the radiance of the background; and τ is the transparency. Thus, I is the integration of the density field along the 3D ray in the interval $[0, L]$. Two steps must be performed using (1) to effectively reconstruct flame density. The target object candidate region must be first estimated, corresponding to estimating L, and then the density field is recovered from reference image intensities, inferring $D(t)$.

Most previous approaches to estimate the flame density field, have been focused on representing the relationship between 3D volumetric data and its projected images, and iteratively reducing the error using a loss function. Density sheet decomposition and computed tomography (CT) based approaches have provided accurate and robust results [10]. However, density sheet decomposition based 3D flame estimation [11] requires considerable computation for decomposition and reconstruction, yet still has problems with estimating realistic smooth shapes because a convex combination of polytopes is still a polytope, hence density sheet decomposition based 3D flame remains in a polytope. Ihrke and Magnor [10] applied CT based techniques for flame reconstruction using a least square method (LSM) based loss function. However, energy based LSM loss functions exhibit unacceptable blurring for iterative reconstruction.

In this paper, we propose a 3D density field estimation of the flame, which formulates the relationship of the image intensity and voxels on the 3D lays by formulating the compact linear combination of atoms using an overcomplete basis. The main contribution of this paper is the proposed multiple image based 3D flame density estimation using compressive sensing, which offers the following advantages.

- The relationship between the 3D flame and its projected multiple images is formulated using discrete and linear equations to effectively recover the 3D density field. This approach simplifies reconstruction, obtains the whole 3D density field in one step, and enables reconstructing realistic smooth shapes rather than polytopes.
- The proposed 3D reconstruction technique uses compressive sensing, enabling reconstruction of large but sparse density fields from a limited number of non-adaptive linear measurements.
- The estimated 3D density field of the flame using compressive sensing reduces the blurring effect arising from notably few flame images and the least squares loss function. In this proposal, we use the loss function balancing trade-off between the closeness (or the fitting) to the data and the sparsity constraint. The sparsity regularization term is added to prevent the blurring while iteration.

The remainder of this paper is organized as follows. Section 2 reviews related image based 3D reconstruction studies, and Section 3 explains the proposed method to reconstruct the flame. Section 4 present experiment results from multiple flame images, and Section 5 summarize and concludes the paper.

II. RELATED WORK

Image based 3D scene reconstruction has been widely studied over the past 30 years, with remarkable results in computer graphics and vision areas. 3D scene reconstruction based on multiple images commenced with stereo vision based approaches [12]. Okutomi and Kanade [13] extended stereo vision based 3D reconstruction to multiple cameras and provided virtual reality using multiple view video acquisition and 3D rendering [14]. Kang *et al.* [15] proposed a multiple view stereo reconstruction method from images with large occlusions. However, these methods were designed to reconstruct depth maps from particular viewpoints, and hence were not suitable for full 3D scene reconstruction from images obtained from multiple surrounding cameras. Image based visual hull reconstruction [16] allowed real-time 3D scene reconstruction from multiple view images, where the algorithm does need not solve the correspondence problem, but simply calculates the convex hull of the silhouettes in all view images.

Although the visual hull method is robust when the cameras surround the object, a concave object cannot be reconstructed using only silhouettes. This problem was solved by a voxel coloring method [17]. Subsequently, numerous multiple image based 3D reconstruction approaches have been proposed for surface reconstruction and free-viewpoint rendering from multiple view video acquisition in controlled indoor studio environments [18]–[21]. The basic principle for volumetric reconstruction is to find a classification for all elements in a discretized volume to describe if they belong

to the surface of the 3D object using spatial appearance and geometric detail information [22]. The fundamental concept of photo consistency is that only voxels that intersect the object's surface have consistent appearance in the various input images, whereas other voxels project to incompatible image patches. Voxel carving by estimating photo consistency simplifies geometric reconstruction, but requires many input images to achieve photo realistic rendering. It is also effective to reconstruct opaque object surfaces, but is unsuitable to reconstruct flame, because it must reconstruct the surface and inner volume of the target object.

Thus, 3D reconstruction and adequate rendering of semitransparent objects, such as fire or smoke, remain open problems in computer graphics. Some approaches extended surface reconstruction techniques considering transparency [23]. Computerized tomography (CT) methods are specialized for the ill-posed situation of sparse views, and employ various techniques to regularize the problem, including favoring local smoothness in a statistical framework, assuming prior shape models, and coarsely discretizing density levels [24], [25]. Hasinoff and Kutulakos [11] developed a spatially compact basis to reconstruct the density field that also enabled convex representation of the density field. Their method provided an efficient 3D reconstruction of fire with only few images.

Sparse signal representation has been recently shown as a powerful tool to acquire, represent, and compress high dimensional signals, and efficiently reconstruct the signal. Mathematically, solving a sparse representation and learning involve seeking the sparsest linear combination of basis functions from an over-complete dictionary. The basic concept to represent or reconstruct signals with sparse samples has extremely important application for many practical fields, such as signal processing, machine learning, computer vision, and robotics [26].

Compressive sensing is based on the principle that signal sparsity can be used to recover the original signal from significantly fewer samples than required by the Shannon-Nyquist theorem [27]–[29]. Compressive sensing algorithms generally include three basic components: sparse representation, encoding measuring, and reconstruction algorithm. In particular, sparse representation approximately solves a system of equations with sparse vectors, and has been widely applied to pattern recognition, because it uses linear combinations of training samples to represent the test sample and compute sparse representation coefficients of the linear representation system.

III. THREE-DIMENSIONAL DENSITY RECONSTRUCTION USING COMPRESSIVE SENSING

This study proposes a density field reconstruction method $D(x) = (\phi_R(x), \phi_G(x), \phi_B(x))$ for a 3D frame object using its 2D projection images $\{I_j\}_{j=1}^{K}$ captured from K preassigned cameras. We regard each projected image, I_j, to be defined on a region $I_j(\Omega)$ in $\mathbb{R}^3$, called the silhouette (region) of I_j). As shown in Fig. 1, the relationship between 3D flame and its

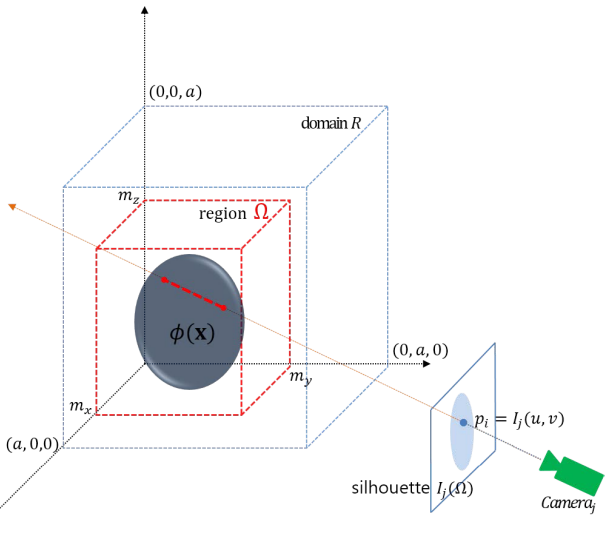

FIGURE 1. Flame in a 3D scene and the projected images. The proposed approach estimates the density field component $\phi(x)$ using the projected intensity values of multiple images.

projected images are represented using its camera calibration data within 3D candidate region. We simplify the process by reconstructing the 3D density component functions $\phi(x, y, z)$ of $D(x, y, z)$ wholly rather than separately computing the epipolar plane $\phi(x, y, z_0)$ for each z_0. We recover $D(x)$ by solving compressive sensing (as given in (6), below) to avoid blurring in reconstruction.

Therefore, flame image based 3D reconstruction is separated into two steps, explained in detail in subsequent sections.

1) Search the target object 3D candidate region, $\Omega \subset R$, from silhouette images, $I_j(\Omega)$, of the flame to reduce computational cost by reducing the number of unknown variables.
2) Estimate the flame density field using compressive sensing to recover a relatively sparse density field from a limited number of intensity measurements.

A. NOTATION AND TERMINOLOGY

For clarity, Table 1 summarizes the mathematical symbols and notations employed in the reconstruction process. Lower case letters are employed for real variables or real valued functions; and upper case letters for multi-dimensional terms, such as images and domains. Constants are generally presented as lower case Greek letters, and vectors are assumed to be columnar, and presented in boldface. However, we denote dimension related constants as K, N, and M.

B. THREE-DIMENSIONAL ESTIMATION OF FLAME CANDIDATE REGIONS

To recover any density function component, ϕ, of the density field, $D(x)$, we simply initiate the bounding box R of the 3D flame, as shown in Fig. 1. However, R contains many points unrelated to frame density, which increases computation size (i.e., the number of unknowns in (4)). To effectively

TABLE 1. Symbols and notations for reconstruction.

Symbol	Description
$\mathbb{R}^3$	3D Euclidean space
$R \subset \mathbb{R}^3$	density function domain
$\Omega \subset R$	region containing density function supports
$I_j\ (j = 1, \ldots, K)$	2D images captured from the j-th camera with size $c \times d$
$I_j(\Omega) \subset \mathbb{R}^3\ (j = 1, \ldots, K)$	silhouette region of I_j
$\Omega_j \subset R$	region in R projected onto $I_j(\Omega)$ by C_j
l_i	rays from cameras to the pixels through R
$D(x)$	3D semitransparent object density field
$\phi = \phi_R, \phi_G, \phi_B$	scalar density function D components
$A = (a_{ik})$	$N \times M$ binary matrix
C_j	perspective projection onto image plane I_j
$\Phi \in \mathbb{R}^M$	density function related vector
$\Psi \in \mathbb{R}^M$	photo consistent density function related vector
$P \in \mathbb{R}^N$	measured pixel value related vector
$x = (x, y, z)$	3D domain variables for density functions
u, v	2D camera captured image variables
p_i	image I_j pixel values
K	number of cameras (or captured 2D images)
$N = K \cdot c \cdot d$	number of measured pixel values
M	volume of region Ω or number of voxels to be reconstructed
$a, m_x, m_y, m_z, \lambda$	constants
$\|\cdot\|_{\ell_0}$	pseudo-norm counting the number of nonzero components in the vector
$\|\cdot\|_{\ell_1}$	Euclidean ℓ_1 norm
$\|\cdot\|_{\ell_2}$	Euclidean ℓ_2 norm
$\cdot^T$	transpose operator

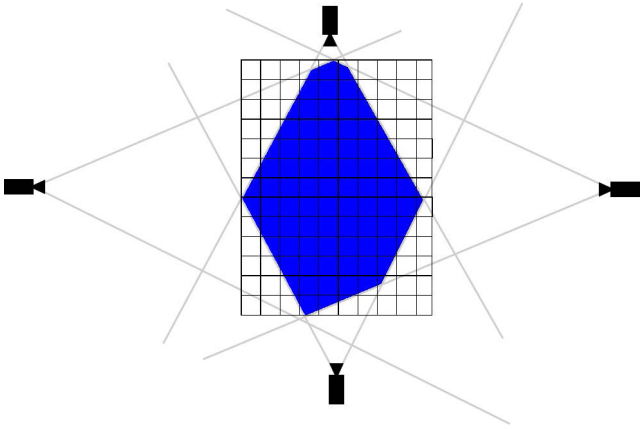

FIGURE 2. Three-dimensional candidate region estimation from the intersection of possible cones containing the object.

estimate the 3D density field, we must reduce the computational domain by estimating the flame distribution candidate region, Ω.

The procedure to estimate Ω starts by finding the 3D related region from each projected image plane $I_j, j = 1, \ldots, K$. Let C_j be the perspective projection for the image plane I_j with corresponding silhouette region $I_j(\Omega) \subset \mathbb{R}^3$. Then, consider the inverse region

$$\Omega_j = \{x \in R : C_j x \in I_j(\Omega)\} = \bigcup_{z \in I_j(\Omega)} C_j^{-1} z,$$

where $j = 1, \ldots, K$; and $C_j^{-1} z$ denotes the line segment in R such that $C_j(x) = z$. Then we construct Ω by intersecting all subregions Ω_j, as shown in Fig. 2,

$$\Omega = \bigcap_{j=1}^{K} \Omega_j = \{x \in R : C_j x \in I_j(\Omega), j = 1, \ldots, K\}.$$

In practice, a discrete version of Ω is commonly obtained by intersecting the cones generated by back projecting the object silhouettes [16], [30].

C. THREE DIMENSIONAL DENSITY ESTIMATION USING COMPRESSIVE SENSING

The 3D density field estimation of the flame within a 3D candidate region Ω is extracted from the information of the pixel intensities from multiple projected images I_j around the target object in Ω. Inevitably, this method gives rise to the under-determined system because the number (M) of the unknown variables $\phi(x)$ for $x \in \Omega$ is much greater than that (N) of known pixel values. That is, the relationship between the projected image and the density field of the semitransparent object in Fig. 1 can be formulated with $N << M$ as in Fig. 3. Numerous approaches have been proposed to solve the under-determined system.

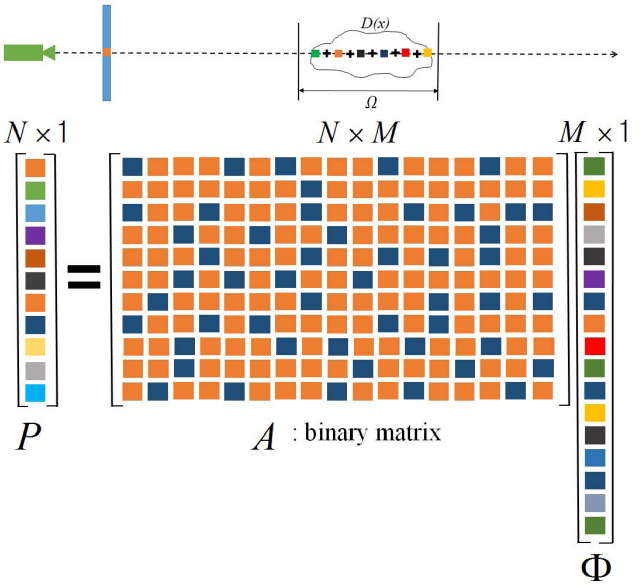

FIGURE 3. A semitransparent object in a three-dimensional scene and corresponding projected images. The proposed approach estimates the density field, *D(x)*, using the projected intensities for multiple images.

Since the computation domain Ω was obtained by silhouette back projection, $\phi(x)$ has zero density for many points $x \in \Omega$. Therefore, $\phi(x)$ values are sparse in Ω, which is a required property for ϕ. The sparse representation method for under-determined systems finds the sparsest solution, uniquely recovered by solving a convex optimization with the smallest l_1 norm when ϕ is somewhat sparse. Sparse representation and compressive sensing provide a rigorous mathematical framework to reconstruct the signal by finding solutions to under-determined linear systems [27]. This method is based on the principle that signal sparsity can be exploited through optimization to recover from significantly fewer samples than required by Shannon-Nyquist sampling. Thus, we estimate the density field of the semitransparent object using the pixel intensities of the projected images,

based on compressive sensing, providing an effective solution of the under-determined system.

Let us consider the proposed case in detail. We want to reconstruct the flame 3D density field $D(x) = (\phi_R(x), \phi_G(x), \phi_B(x))$ using K simultaneously captured 2D images $I_j(u, v)$ of size $c \times d$. Since the dynamic object is not a large, thick target, and is captured at relative close distance, we may simplify model (1) by assuming that $J(x)$ is constant self-emission, and transparency $\tau(x)$ remains constant, which are commonly provided in existing literature on combustion analysis (see [11] and references therein). Background radiance, I_{bg}, is also preassigned, so we treat this as a zero image by absorbing it into I. We may assume some transformation for (1) such that the intensity at pixel p of I related to each component $\phi(x)$ of $D(x)$ becomes ([11])

$$I_p = \int_0^L \phi(t)\, dt, \tag{2}$$

and we discretize (2) component by component to provide $N = K \cdot c \cdot d$ linear equations,

$$p_i = \int_{l_i} \phi(x) dx = \sum_{x \in l_i} \phi(x), \quad i = 1, \ldots, N, \tag{3}$$

where, each l_i is a ray from a camera to a pixel point through region $R = \{x = (x, y, z) \in \mathbb{R}^3 : 0 \le x, y, z \le a\}$, where ϕ is defined. Since the particles of a dynamic object, such as flame or smoke, stay together and continuously move, we assume that ϕ has a compact support $\{x \in R : \phi(x) \neq 0\}$ inside a region $\Omega \subseteq \{x = (x, y, z) \in R : 0 \le x < m_x, 0 \le y < m_y, 0 \le z < m_z\}$, such that $\phi(x)$ is nonnegative at each voxel $x \in \Omega$ and zero outside Ω.

Thus, we number the points in Ω as $\{x_k\}_{k=1}^M$ and represent (3) using vector notation as

$$A\Phi = P \tag{4}$$

where $P = (p_1, \ldots, p_N)^T$; $\Phi = (\phi(x_1), \ldots, \phi(x_M))^T$; and $A = (a_{ik})$ is an $N \times M$ binary matrix,

$$a_{ik} = \begin{cases} 1, & \text{if } x_k \in l_i \cap \Omega \\ 0, & \text{otherwise.} \end{cases} \tag{5}$$

Since we simultaneously obtain projected images from a few cameras, the system is under-determined ($N < M$), so there can be infinitely many solutions to (4), called the photo consistent density field [11]. Before we attempt to find a solution, we closely examine (4) and related terms. From (5), all entries of A are either zero or one, i.e., A is a binary matrix, and the unknown vector Φ originates from the density function $\phi(x)$, hence all components are nonnegative. The support set of $\phi(x)$, i.e., the semitransparent objects shape, is within Ω, and is relatively small compared to the Ω domain; thus, the vector Φ is sparse. We reconstruct the density function ϕ by considering all cases, and the nonnegative LARSE-LASSO algorithm ([31]–[33]) to solve the

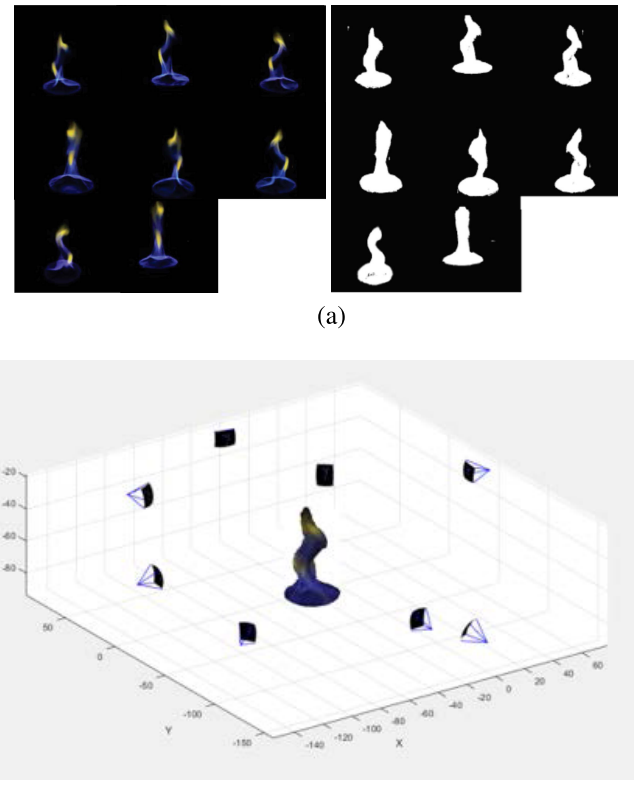

(a)

(b)

FIGURE 4. Experimental setup for three-dimensional (3D) reconstruction of semitransparent objects by capturing multiple images of flame and smoke. From left to right: captured images, silhouette images, and camera calibration data. (a) Flame images and corresponding silhouette images using background subtraction. (b) 3D candidate region using image based visual hull and 3D camera positions.

nonnegative sparse constrained optimization

$$\begin{aligned} &\underset{\Psi \in \mathbb{R}^M}{\text{argmin}} \ \|A\Psi - P\|_{\ell_2}^2 + \lambda \|\Psi\|_{\ell_1}, \\ &\text{constrained to} \quad \Psi \ge 0, \end{aligned} \tag{6}$$

where $\Psi \ge 0$ indicates that all components of Ψ are nonnegative.

We consider the suitability and effectiveness of the proposed nonnegative sparse optimization to reconstruct $D(x)$. In (6), $\|A\Psi - P\|_{\ell_2}$ is related to the ℓ_2-norm and controls photo consistency to density and global fitness. The second term enables the reconstructed density to be sparse, because the ℓ_1-norm is a well-known successful alternative of the ℓ_0- pseudo norm ([27], [34] and references therein). Nonnegative sparse optimization and nonnegative matrix factorization have been shown to be empirically successful in extracting meaningful features from a diverse collection of real-life data sets [35]. Nonnegative sparse optimization has also been widely considered in machine learning, pattern recognition and computer vision models ([36]–[39]). Sparsity reflection by the ℓ_1 penalty term with nonnegative constraints implies the minimized ℓ_0-norm of the histogram of the reconstructed images, and avoids scattering and blurring of the reconstructed images.

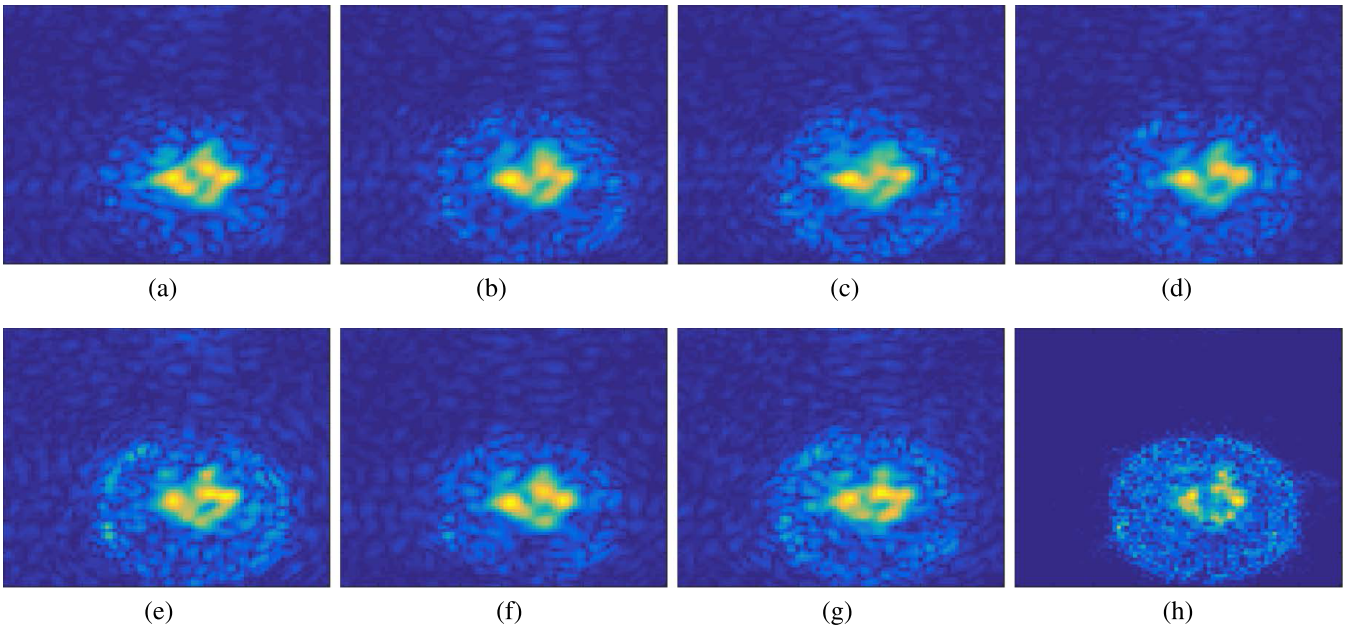

FIGURE 5. Visualizatioin of the proposed CS based flame density fields estimation procedure, in successive steps numbered from 1 to 1600. Subimages represent the estimated density fields from top view in every 200 iteration steps. (a) iteration # 200. (b) iteration # 400. (c) iteration # 600. (d) iteration # 800. (e) iteration # 1000. (f) iteration # 1200. (g) iteration # 1400. (h) iteration # 1600.

This approach simplifies the reconstruction process by obtaining the whole 3D density field in a single step rather than separately computing epipolar planes parallel to an axis, as required in the density sheet decomposition method [11]. This enables us to reconstruct a realistic smooth shape rather than a polytope obtained from the density-sheet decomposition, which is a major advantage because a convex combination of polytopes remains a polytope.

Updating the semitransparent object density field using CS, the nonnegative sparse optimization enables reconstructing the optimal 3D density by reducing blurring compared to previous solutions for under-determined systems, such as the algebraic reconstruction technique (ART) [40].

IV. EXPERIMENTAL RESULTS

Section IV-A discusses the experimental for the proposed image based flame 3D reconstruction, and Section IV-B reports 3D reconstruction using the proposed approach for multiple captured images.

A. EXPERIMENTAL SETUP

We demonstrate the robustness and effectiveness of the proposed approach using image sequences captured from a natural environment. The fire image sequences have 320 × 240 pixel resolution, include camera calibration, and were captured from eight convex positions around the target object. Figure 4 shows the captured and silhouette images used to find the flame 3D candidate region (Fig. 4(a)). The candidate region was estimated using its input RGB images, silhouette images, and camera calibration data, as shown in Fig. 4(c)). The proposed method was implemented in MATLAB and evaluated on a PC with Intel(R) Core^{TM} i7-7700 CPU (3.66GHz), 16 GB RAM.

B. THREE-DIMENSIONAL RECONSTRUCTION EVALUATION

The proposed CS based density field estimation was evaluated in various views to validate robustness. Flame 3D density fields were estimated from flame 3D candidate regions produced from photo consistency-based voxel carving using projected images, silhouette images, and camera calibration data. We estimated and visualized the density fields within the candidate region in the projected arbitrary view, using (1) to quantitatively evaluate performance.

First, we demonstrate how the 3D density fields can be iteratively updated using CS within the candidate region. Figure 5 represents projected 3D density fields from a top view according to its iteration. The 3D density fields are meaningless after only a few iterations, but this is updated using the relationship between the reference image intensities and the 3D density fields. Flame boundary and background are more clearly represented and deblurred with increasing iterations. The loss function for sparse reconstruction is composed of fitting term and sparse regularization terms, as shown in (6). Experimentally, the loss function is optimized by iteration 1600. This result stems from the fact that the sparse recovery generates images with its density sparse or concentrated in a small subregion [41], [42] (also see [43] and references therein). That is the reconstructed density ϕ has the property that the supporting set $\{x \in \Omega : \phi(x) \neq 0\}$ or its histogram $\{\phi(x) : x \in \Omega\}$ is small in its set size and there exists a small subset $K \subset \Omega$ such that

$$\sum_{x\in\Omega} \phi(x)^2 = \sum_{x\in K} \phi(x)^2 \quad \text{or} \quad \sum_{x\in\Omega} \phi(x)^2 \approx \sum_{x\in K} \phi(x)^2.$$

As shown in Fig. 5, the reconstruction performance reflect well this property, gradually generating approximations in which the blurring disappear and become clear.

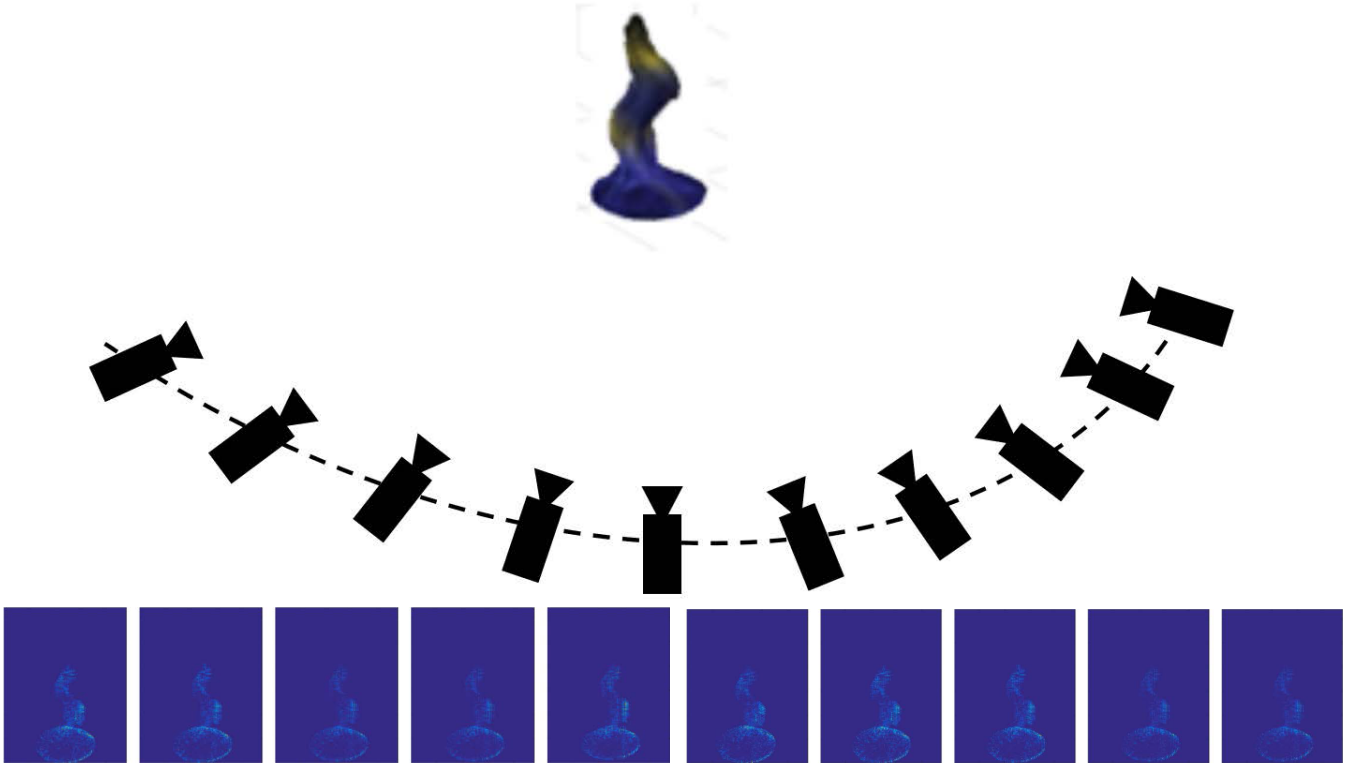

FIGURE 6. Estimated density fields of the flame at the various arbitrary views which are reconstructed from few reference images. The density fields at an arbitrary views are estimated using camera calilbration data and its 3D density fields.

Secondly, we then represent the density field reconstruction outcomes in an arbitrary view. Figure 6 shows the density fields projected into 10 different viewpoints. The 3D density fields are projected using its camera perspective projection matrix of the image and the 3D density fields from (3) to visualize the reconstructed 3D density fields. Our CS based flame 3D density fields are estimated by constructing optimized linear combination of the 3D scene and projected images by minimizing the object function. Apart from photo consistency-based density fields estimation [11], our flame 3D density fields estimation is less dependent on the number of views and camera geometry, we can effectively reconstruct the flame density fields at an arbitrary viewpoint.

Lastly, we use only seven images among the eight reference images to reconstruct the density fields in the viewpoint of the eighth reference image, to validate the proposed CS based 3D flame reconstruction, and compare the reconstructed density fields with the original eighth reference image, to validate the robustness of the proposed CS based 3D reconstruction of flame, as shown in Fig. 7. The reconstructed shape and density are very similar to the original reference flame image. It is worth noting that the proposed method is less affected by the initial camera position and reconstructs a realistic smooth shape because we reconstruct the whole density function $\phi(x, y, z)$ in a single process rather than by generating each density sheet $\phi(\cdot, \cdot, z)$ for each z and merging them to build the whole body.

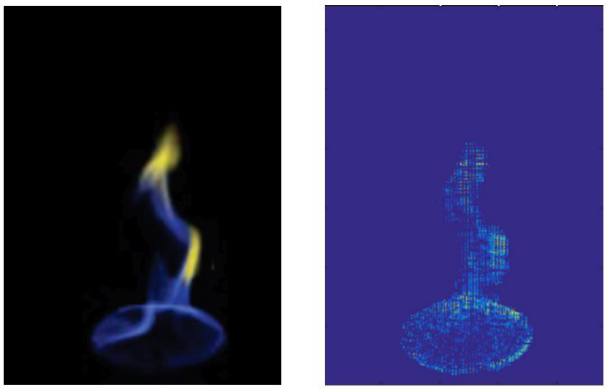

FIGURE 7. Comparison of the projected image and its density fields using our proposed approach at an arbitrary viewpoint to show the robustness of the proposed approach.

V. DISCUSSION

This paper proposes a density field estimation of complicated 3D structure of the flame from multiple projected images captured around the flame. The proposed non-parametric 3D reconstruction using CS shows robustness in reconstructing the original shape without prior information of the target object, and requires only a small number of linear measurements.

We propose that the reconstruction method based on CS using flame's images is often represented in terms of only a

few data pixel values in the spatial domain using the effective loss function, composed of cost and sparsity regularization terms. The CS based flame 3D density fields reconstruction approach is less dependent on the number of projections collected around the target object, allowing the original shape to be recovered with only a few measurements by preserving sparsity. Experimental validation shows the proposed method is very effective to reduce blurring effects within the flame and preserve the boundary between flame and background.

This method can be applied to realistically visualize smoke or fire evolution. In modeling the flame evolution, most researchers have used the Navier-Stokes (NS) equation. To effectively solve solutions in accordance with reality, the initial shape (the domain for the NS equation) is sensitive, so we are required to initialize the shape as close as possible to the actual data. Thus, our proposed flame 3D density fields estimation and reconstruction can be applicable for the data assimilation in modeling fire or smoke from a few still image sequences.

REFERENCES

[1] Z. Luo and H. C. Zhou, "A combustion-monitoring system with 3-D temperature reconstruction based on flame-image processing technique," *IEEE Trans. Instrum. Meas.*, vol. 56, no. 5, pp. 1877–1882, Oct. 2007.

[2] G. Gilabert, G. Lu, and Y. Yan, "Three-dimensional tomographic reconstruction of the luminosity distribution of a combustion flame," *IEEE Trans. Instrum. Meas.*, vol. 56, no. 4, pp. 1300–1306, Aug. 2007.

[3] G. Lu, Y. Yan, and M. Colechin, "A digital imaging based multifunctional flame monitoring system," *IEEE Trans. Instrum. Meas.*, vol. 53, no. 4, pp. 1152–1158, Aug. 2004.

[4] S. H. Chung, "Several applications of laser diagnostics for visualization of combustion phenomena," *J. Vis.*, vol. 6, no. 2, pp. 95–106, 2003.

[5] P. Ewart and B. Williams, "Laser-based measurements of combustion engines—Inside and outside," in *Proc. Frontiers Opt.*, 2017, pp. 1–2.

[6] A. Khatamian and H. R. Arabnia, "Survey on 3D surface reconstruction," *Proc. JIPS*, vol. 12, no. 3, pp. 338–357, 2016.

[7] J. R. Frisvad, N. J. Christensen, and P. Falster, "Efficient light scattering through thin semi-transparent objects," in *Proc. ACM GRAPHITE*, D. Arnold and M. Billinghurst, Eds. New York, NY, USA: Association for Computing Machinery, 2005, pp. 135–138.

[8] M. Borga and H. Knutsson, "Estimating multiple depths in semi-transparent stereo images," in *Proc. SCIA*, 1999, p. 3.

[9] O. Mishchenko and R. Crawfis, "On perception of semi-transparent streamlines for three-dimensional flow visualization," *Comput. Graph. Forum*, vol. 33, no. 1, pp. 210–221, 2014.

[10] I. Ihrke and M. Magnor, "Image-based tomographic reconstruction of flames," in *Proc. ACM SIGGRAPH/Eurogr. Symp. Comput. Animation* 2004, pp. 367–376.

[11] S. W. Hasinoff and K. N. Kutulakos, "Photo-consistent reconstruction of semitransparent scenes by density-sheet decomposition," *IEEE Trans. Pattern Anal. Mach. Intell.*, vol. 29, no. 5, pp. 870–885, May 2007.

[12] D. Marr and T. Poggio, "A theory of human stereo vision," Artif. Intell. Lab. (Memo. 451), Massachusetts Inst. Technol., Cambridge, MA, USA, 1977.

[13] M. Okutomi and T. Kanade, "A multiple-baseline stereo," *IEEE Trans. Pattern Anal. Mach. Intell.*, vol. 15, no. 4, pp. 353–363, Apr. 1993.

[14] T. Kanade, P. Rander, and P. J. Narayanan, "Virtualized reality: Constructing virtual worlds from real scenes," *IEEE Multimedia*, vol. 4, no. 1, pp. 34–47, Jan. 1997.

[15] S. B. Kang, R. Szeliski, and J. Chai, "Handling occlusions in dense multi-view stereo," in *Proc. CVPR*, 2001, pp. I-103–I-110.

[16] W. Matusik, C. Buehler, L. McMillan, R. Raskar, and S. J. Gortler, "Image-based visual hulls," in *Proc. Comput. Graph. Conf. (SIGGRAPH)*, S. Hoffmeyer, Ed. New York, NY, USA: ACM Press, 2000, pp. 369–374.

[17] S. M. Seitz and C. R. Dyer, "Photorealistic scene reconstruction by voxel coloring," *Int. J. Comput. Vis.*, vol. 35, no. 2, pp. 151–173, 1999.

[18] T. Matsuyama, X. Wu, T. Takai, and S. Nobuhara, "Real-time 3D shape reconstruction, dynamic 3D mesh deformation, and high fidelity visualization for 3D video," *Comput. Vis. Image Understand.*, vol. 96, pp. 393–434, Dec. 2004.

[19] L. Zitnick, S. B. Kang, M. Uyttendaele, S. Winder, and R. Szeliski, "High-quality video view interpolation using a layered representation," *ACM Trans. Graph.*, vol. 23, no. 3, pp. 600–608, Aug. 2004.

[20] Y. Furukawa and J. Ponce, "Accurate, dense, and robust multiview stereopsis," *IEEE Trans. Pattern Anal. Mach. Intell.*, vol. 32, no. 8, pp. 1362–1376, Aug. 2008.

[21] E. de Aguiar, C. Stoll, C. Theobalt, N. Ahmed, H.-P. Seidel, and S. Thrun, "Performance capture from sparse multi-view video," *ACM Trans. Graph*, vol. 27, no. 3, pp. 98-1–98-10, 2008.

[22] H. P. A. Lensch, J. Kautz, M. Goesele, W. Heidrich, and H.-P. Seidel, "Image-based reconstruction of spatial appearance and geometric detail," *ACM Trans. Graph.*, vol. 22, no. 2, pp. 234–257, 2003.

[23] J. De Bonet and P. Viola, "Roxels: Responsibility weighted 3D volume reconstruction, " in *Proc. ICCV*, 1999, pp. 418–425.

[24] S. B. Xu and W. X. Lu, "Surface reconstruction of 3D objects in computerized tomography," *Comput. Vis., Graph. Image Process.*, vol. 44, pp. 270–278, Dec. 1988.

[25] G. T. Herman, *Fundamentals of Computerized Tomography: Image Reconstruction from Projections*. London, U.K.: Springer-Verlag, 2009.

[26] R. G. Baraniuk, E. Candes, M. Elad, and Y. Ma, "Applications of sparse representation and compressive sensing [Scanning the Issue]," *Proc. IEEE*, vol. 98, no. 6, pp. 906–909, Jun. 2010.

[27] D. L. Donoho, "Compressed sensing," *IEEE Trans. Inf. Theory*, vol. 52, no. 4, pp. 1289–1306, Apr. 2006.

[28] E. J. Candès and M. B. Wakin, "An introduction to compressive sensing," *IEEE Signal Process. Mag.*, vol. 25, no. 2, pp. 21–30, Mar. 2008.

[29] R. G. Baraniuk, "Compressive sensing," *IEEE Signal Process. Mag.*, vol. 24, no. 4, pp. 118–121, Jul. 2007.

[30] A. Laurentini, "The visual hull concept for silhouette-based image understanding," *IEEE Trans. Pattern Anal. Mach. Intell.*, vol. 16, no. 2, pp. 150–162, Feb. 1994.

[31] B. Efron, T. Hastie, I. Johnstone, and R. Tibshirani, "Least angle regression," *Ann. Statist.*, vol. 32, no. 2, pp. 407–499, 2004.

[32] M. Morup, K. H. Madsen, and L. K. Hansen, "Approximate L_0 constrained non-negative matrix and tensor factorization," in *Proc. IEEE Int. Symp. Circuits Syst.*, May 2008, pp. 1328–1331.

[33] R. Tibshirani, "Regression shrinkage and selection via the lasso," *J. Roy. Statist. Soc. B, Methodol.*, vol. 58, no. 1, pp. 267–288, 1996.

[34] A. M. Bruckstein, M. Elad, and M. Zibulevsky, "On the uniqueness of nonnegative sparse solutions to underdetermined systems of equations," *IEEE Trans. Inf. Theory*, vol. 54, no. 11, pp. 4813–4820, Nov. 2008.

[35] P. O. Hoyer, "Non-negative matrix factorization with sparseness constraints," *J. Mach. Learn. Res.*, vol. 5, pp. 1457–1469, Dec. 2004.

[36] R. He, B. Hu, W.-S. Zheng, and Y. Guo, "Two-stage sparse representation for robust recognition on large-scale database," in *Proc. 24th AAAI Conf. Artif. Intell. (AAAI)*, 2010, pp. 475–480.

[37] R. He, W.-S. Zheng, B.-G. Hu, and X.-W. Kong, "Nonnegative sparse coding for discriminative semi-supervised learning," in *Proc. IEEE Comput. Soc. Conf. Comput. Vis. Pattern Recognit.*, Jun. 2011, pp. 2849–2856.

[38] Y. Ji, T. Lin, and H. Zha, "Mahalanobis distance based non-negative sparse representation for face recognition," in *Proc. Conf. Mach. Learn. Appl. (ICMLA)*, 2009, pp. 41–46.

[39] N. Vo, B. Moran, and S. Challa, "Nonnegative-least-square classifier for face recognition," in *Proc. 6th Int. Symp. Neural Netw. Adv. Neural Netw.*, 2009, vol. 58, no. 1, pp. 449–456.

[40] E. Grossmann, D. Ortin, and J. Santos-Victor, "Algebraic aspects of reconstruction of 3D scenes from one or more views," in *Proc. BMVC*, 2001, pp. 633–642.

[41] E. J. Candés, J. K. Romberg, and T. Tao, "Stable signal recovery from incomplete and inaccurate measurements," *Commun. Pure Appl. Math.*, vol. 59, no. 8, pp. 1207–1223, 2006.

[42] J. A. Tropp, "Greed is good: Algorithmic results for sparse approximation," *IEEE Trans. Inf. Theory*, vol. 50, no. 10, pp. 2231–2242, Oct. 2004.

[43] A. C. Gilbert, M. Muthukrishnan, and M. J. Strauss, "Approximation of functions over redundant dictionaries using coherence," in *Proc. 14th Annu. ACM-SIAM Symp. Discrete Algorithms*, 2003, pp. 243–252.

GANG-JOON YOON received the M.S. and Ph.D. degrees in mathematics from the Korea Advanced Institute of Science and Technology, in 1995 and 1999, respectively. He is currently a Researcher with the National Institute for Mathematical Sciences, South Korea, and a member of the National Agenda Project of Korea on Surveillance Systems. His research interests include compressive sensing and computer vision based on mathematics and functional analysis.

HYEYOUN CHO received the M.S. degree in computer science from Kookmin University, Seoul, South Korea, in 2018. Her current research interests include image-based 3D reconstruction, deep learning-based classification, and its applications.

YONG-YUK WON (M'08) received the B.S., M.S., and Ph.D. degrees in electrical and electronic engineering from Yonsei University, Seoul, South Korea, in 1997, 1999, and 2008, respectively. From 1999 to 2002, he was with the Optoelectronics Lab, Samsung Electronics, where he was involved in research and development on optical devices. He is currently an Assistant Professor with Myongji University, South Korea. His current research interests include passive optical networks, visible light communication, optical devices, and optical systems for communications.

SANG MIN YOON received the B.E. and M.E. degrees in electronics engineering from Korea University, Seoul, South Korea, in 2000 and 2002, respectively, and the Dr.Ing. degree in computer science from TU Darmstadt, Darmstadt, Germany, in 2010. He did Postdoctoral Research with the Digital Human Research Center, Advanced Industrial Science and Technology, Tokyo, Japan. From 2002 to 2005, he was a Researcher with the Samsung Advanced Institute of Technology, where he was involved in the areas of face recognition and video surveillance. Since 2012, he has been an Associate Professor with the School of Computer Science, Kookmin University, South Korea. He is also a Visiting Researcher with the Department of Mechanical Engineering, MIT. His research interests include computer vision and pattern recognition, including object detection and recognition, visual object tracking, 3D model retrieval, and human–computer interface.